

# An Experimental Insight on the Selection of the Tool Tilt Angle for Friction Stir Welding of 7075 T651 Aluminum Alloys

Pratik H. Shah<sup>1,2</sup> and Vishvesh J. Badheka<sup>3</sup>

<sup>1</sup>Department of Mechanical Engineering, Faculty of Technology, Charusat University, Changa -388421, Gujarat, India

<sup>2</sup>Sardar Vallabhbhai Patel Institute of Technology (SVIT), VASAD - 388306, Gujarat, India; p1shah55@yahoo.com

<sup>3</sup>Department of Mechanical Engineering, School of Technology, Pandit Deendayal Petroleum University, Gandhinagar - 382007, Gujarat, India; vishvesh79@gmail.com

## Abstract

**Objectives:** To determine the optimum tool tilt angle for friction stir welding (FSW) Al 7075-T651 alloy plates by investigating the mechanical and metallurgical properties of the joints. **Methods/Statistical Analysis:** Al 7075-T651 plates of 6.5mm thickness are welded varying the tool tilt angle from 0 to 6 degrees. The mechanical properties like tensile strength and microhardness are evaluated. The testing of tensile specimens is done as per ASTM E8 M-04 standards. The Vickers hardness has been investigated at the weld center in the transverse direction. The microstructural changes occurring are studied with the help of metallographic inspection. Scanning electron microscopy (SEM) has been adopted to evaluate the fracture mode of the tensile specimens. **Findings:** An important welding parameter in FSW that influences the welding quality is the tool tilt angle. In this paper the results of Al 7075-T651 joints welded by FSW with varying tilt angle are investigated for their mechanical strength and metallurgical properties. Evaluation of the tensile strength is carried out and put in relation with the microstructure investigations. From the experimental analysis it is observed that the weld joints made with two degree tool tilt angle are defects free resulting into the best mechanical and metallurgical properties compared to other joints. The fracture surface examination with the scanning electron microscope shows that the fracture surface of the joints are largely governed by the change in the tilt angles. The observations of fracture surface under SEM shows that the joint made with two degree tilt angle failed in a ductile mode whereas all the other joints failed in brittle mode. **Application/Improvements:** 7000 series aluminum alloys are a family of alloys that are practically unweldable by fusion welding processes. FSW procedure can be economically utilized to weld such alloys. This study will benefit to direct the selection of tool tilt angle during FSW of Al 7075 T651 plates.

**Keywords:** Friction Stir Welding, Fractography, Joint Efficiency Tool Tilt Angle, Metallography, Microhardness

## 1. Introduction

Aluminum alloy 7075 have received special attention in industries today due to its high strength. It has been for some time understood that they have an especially very good response to age hardening. The natural aging characteristics along with its high strength to weight ratio, makes it alluring for various aircraft applications<sup>1</sup>. Zinc,

copper and magnesium are the most important alloying elements. This alloy is widely used in manufacturing of air ship components, earth moving equipments and military vehicles<sup>2,3</sup>. The major problem in fusion welding of these alloys is their extremely high sensitivity to solidification cracking. The small amount of copper present in it adds to the problem by extending the coherence range and thus the crack sensitivity. This limits the use of

\*Author for correspondence

the alloy to the applications which needs no fusion welding<sup>4,6</sup>. The process was invented by The Welding Institute (TWI) in 1991. The process is considered to be environmentally clean and energy efficient process. It is widely used to weld light alloys like the aluminium 7xxx series that are practically unweldable by fusion welding processes. FSW takes place at a temperature quite below the melting point of the alloys being joined and makes use of a non consumable tool. The tool is specifically designed to have certain pin features alongwith shoulder features. During the process the tool rotates and the rotating pin is plunged into the adjoining edges of the workpiece to be joined. The welding is done by severe plastic deformation and frictional heating caused by a rotating tool. The collective effect of the tool translation and rotation creates a plastically deformed region resulting into a joint as the tool moves.<sup>9</sup> The major benefits derived of FSW are (i) low distortion, even in long welds (ii) utility with alloys which cannot be fusion welded due to cracking susceptibility and (iii) embedded oxide removal from joint faying surfaces. FSW seems to be one of the most potential techniques for joining aluminum alloy 7075 T651 avoiding the potential problem of solidification cracking. In fusion welding, solidification cracking occurs within the fusion zone and is caused by solidification shrinkage. Such phenomena is not observed with FSW as the process is entirely done in the solid state. The results obtained in the past by joining high strength aviation aluminium alloys with FSW are quite encouraging<sup>4</sup>. Friction stir welding process was used at TWI to weld 7075 T651 aluminum<sup>7</sup>.

The friction stir welding of 7000 series Al alloys has been widely studied by researchers. The microstructural properties of the welds have been studied by<sup>6,8,9</sup>. The mechanical properties have been studied by<sup>1,9-12</sup>. The superplasticity has been studied by<sup>13-16</sup>. The effect on weld quality by PWHT (post weld heat treatment) has been studied by<sup>2,17</sup>. Rajakumar et al.<sup>1</sup> studied the effect of various FSW parameters viz. the welding speed, the axial force

and the tool rotational speed on mechanical properties of FS welded Al-7075 aluminium welded joints. Raja et al.<sup>18</sup> investigated the effect of welding speed on the mechanical properties of friction stir welded aluminium alloy 6061. Mahoney et al.<sup>2</sup> in their studies evaluated the tensile strength of Al 7075 alloy both longitudinally in the weld nugget zone and transverse to the joint. A correlation between the weld parameters and temperatures during welding was established by Reynolds et al.<sup>19</sup> Hatamleh et al.<sup>20</sup> observed formation of onion rings during welding of Al 7075-T351 alloys. Superplasticity of friction stir processed Al 7075-T651 alloy have been studied by Dieguez et al.<sup>13</sup> Patel et al.<sup>14</sup> studied the effect polygonal pin profiles on friction stir processed superplasticity of AA7075 alloy. The effect of various surface heat treatments techniques has been extensively studied by Hatamleh et al.<sup>20,21</sup> Amiri et al.<sup>11</sup> investigated the behavior of microcrack initiation and propagation in Al 7075-T6 by conducting series of fatigue tests. The effects of PWHT on properties of Al 7075-T651 alloy has been investigated by Sivaraj et al.<sup>2</sup> Dhas et al.<sup>22</sup> studied the residual stresses in friction stir welded AA6061-AZ61. The tool tilt angle plays a vital role in defining the weld quality in FSW. A large tool tilt angle tends to lift the tail of the pin from the weld root creating defective welds. Hence it becomes important to select proper tool tilt angle. The work aims at finding the best tool tilt angle for the available welding conditions for 7075-T651 aluminium alloy.

The primary objectives of this investigation are, to study the effect of various tool tilt angles on

- (i) the weld quality, by undertaking detailed mechanical testing of the FS welded AA7075-T651 alloy,
- (ii) the microstructural evolution of the welds,
- (iii) evaluation of the tensile fracture surfaces
- (iv) and thereby to find out the best suited tool tilt angle for the existing experimental conditions.

**Table 1.:** Chemical composition (wt%) of the base metal.

Element	Si	Fe	Cu	Mn	Mg	Zn	Cr	Ti	Al
Base metal (7075 T651)	0.025	0.142	1.21	0.032	2.126	6.045	0.128	0.056	Remainder

**Table 2.** Mechanical properties of the base metal

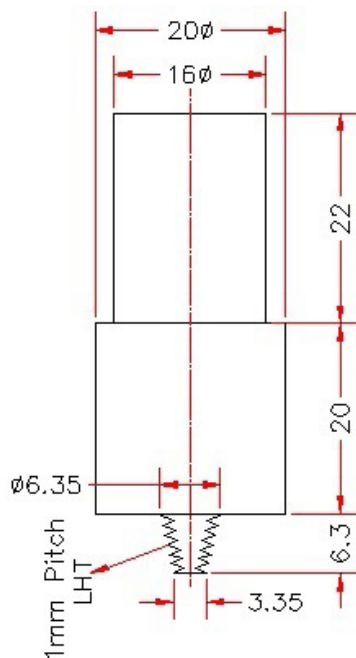
Material	Yield Strength (MPa)	Ultimate Tensile Strength (MPa)	Elongation (%)
Base metal (7075 T651)	510	568	18.3

## 2. Material and Experimental Procedure

Al 7075-T651 alloy plates with a thickness of 6.5 mm were used in the study. The plates of 100 mm X 50 mm were used for the weld trials. The chemical composition of the materials plates used for the study is shown in Table 1. Table 2 depicts the mechanical properties plates. The welding tool used for the investigation is fabricated M2 grade high speed steel. The pin of the tool was machined to have a cylindrical tapered threaded pin feature. Figure 1 shows the dimensions of the tool. The machined tool was heat treated to achieve an hardness of upto 60 HRC. The tool material's composition is shown in Table 3.

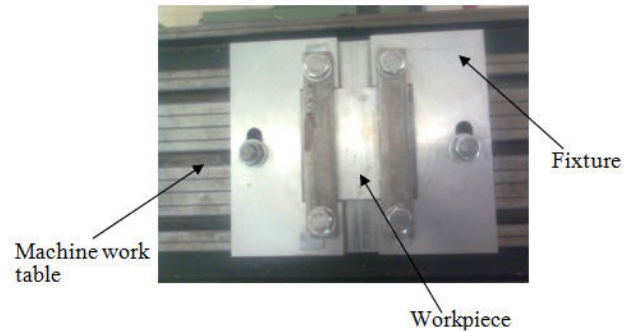
**Table 3.** Chemical composition (wt%) of the tool material

Element	C	Cr	W	Va	Mo
Tool material (HSS)	0.876	4.124	6.411	1.755	4.537



**Figure 1.** The FSW tool.

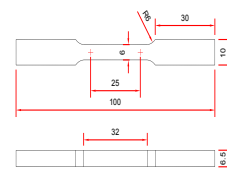
The welding was conducted with the help of a vertical milling machine. Butt joint configuration is used to weld the plates. A specially designed fixture made from SS 304 to rigidly clamp the plates was used during the process. It also did the function of the backing plate. Figure 2. shows the workpieces clamped in the fixture.



**Figure 2.** Workpiece and fixture.

Seven weld joints were prepared with tool tilt angles varying from 0 - 6°. Owing to the uncertainty in FSW weld quality for some parameters which has been observed in the literature, the same set of experiments were repeated. The investigation was performed by different tilt angle keeping various other parameters constant. The values of important FSW parameters like tool travel speed and welding speed were chosen on the basis of optimum values reported in the available literature. The process parameters are presented in Table 4.

The welded specimens were allowed to naturally age for a period of 60 days. After ascertaining that the welds qualify for visual inspection, they were further subjected to mechanical and metallographic investigations. The mechanical testing involved tensile and microhardness measurements. Tensile test specimens were machined using as per ASTM E8 M-04 standards<sup>[11]</sup>. Figure 3 shows the dimensions of the tensile specimen. From each weld coupon three tensile test specimens were extracted.

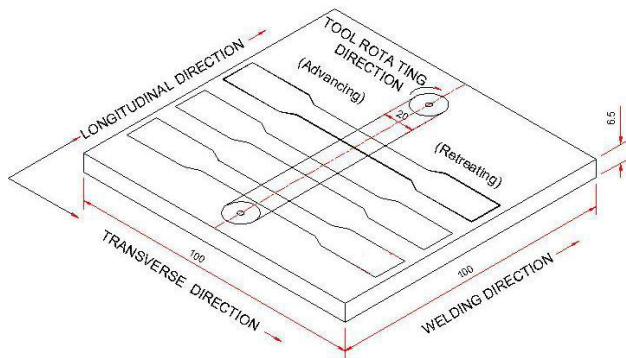


**Figure 3.** Dimensions of tensile specimen as per ASTM E8 M-04 standard (in mm).

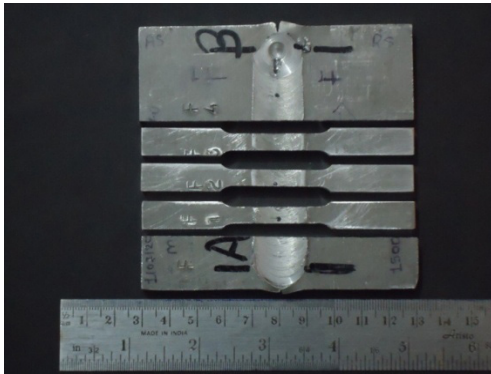
The specimens were normal to the weld line as shown in Figure 4. The average of the three tensile strengths has been reported.

A sample photograph of the tensile specimens prepared for sample F is shown in Figure 5. The tensile testing was done on a computer controlled 20 KN UTM

machine (Make: Tinius Olsen) with 0.5 mm/min constant head speed. The load was applied axially perpendicular to the weld line.



**Figure 4.** Schematic illustration showing the specimen layout to evaluate the tensile strength.



**Figure 5.** Tensile specimens of sample F.

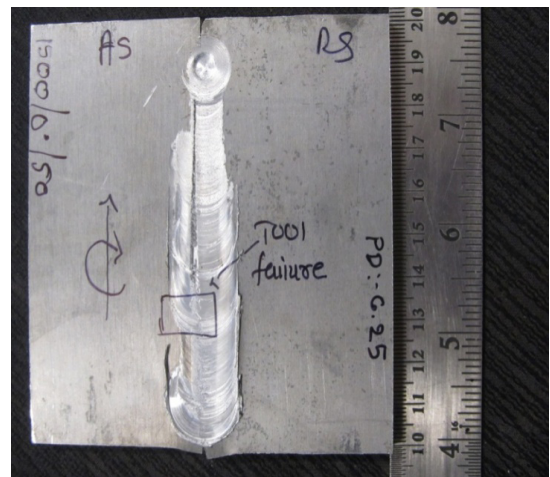
The metallographic investigations were done with the optical microscope (Make: Olympus GX51). The specimens for metallurgical study were cut perpendicular to the weld in required size and standard procedures for preparing metallographic samples were followed. The specimens were first polished manually using different grades of emery papers of silicon carbide. The final polishing was done on a cloth first by using alumina paste followed by diamond paste. This followed final cleaning with acetone and etching with Keller's reagent. A standard Keller's reagent made of 5 ml  $\text{HNO}_3$  (95% concentration), 2 ml HF, 3 ml HCl, 190 ml  $\text{H}_2\text{O}$  was used for the purpose<sup>4</sup>. ESEWAY – Nexus 4302 tester at a load of 300 g for 15 seconds<sup>23</sup> was used to measure the Vickers hardness at the weld center in the transverse direction. The microhardness was measured for a length of 25mm in each samples. A total of twenty five tests each were conducted on the advancing side and the retreating side at an inter-

val of 0.5 mm, with a total of 51 indentations per sample. Finally fracture surface analysis was done using Scanning Electron Microscope (SEM) technique.

## 3. Results and Discussion

### 3.1 Visual Inspection

After welding the test coupons at various tool tilt angles, visual inspection was done to assess the quality of welding. It was observed that the friction stir welding done at  $0^\circ$  tool tilt angle resulted in the failure of the tool pin at the pin-shoulder interface. Figure 6 shows the pin failure inside the workpiece. The coupon welded with  $1^\circ$  tool tilt angle clearly showed weak or intermittent linking on the surface of the weld. Figure 7 shows the picture of test coupon welded at  $1^\circ$  tool tilt angle. The trials for  $0^\circ$  and  $1^\circ$  tool tilt angle were repeated but the welds were unsatisfactory. Hence coupons welded with  $0^\circ$  and  $1^\circ$  tool tilt angles do not qualify for further investigations. The visual inspection of all the test coupons welded with  $2^\circ$ ,  $3^\circ$ ,  $4^\circ$ ,  $5^\circ$  and  $6^\circ$  tool tilt angles showed acceptable quality of weld without any marked visual defects. Hence it was decided to go for further investigations of the joints welded with  $2^\circ$ ,  $3^\circ$ ,  $4^\circ$ ,  $5^\circ$  and  $6^\circ$  tilt angles.



**Figure 6.** Test coupon welded at  $0^\circ$  tool tilt angle.

### 3.2 Microstructure Analysis

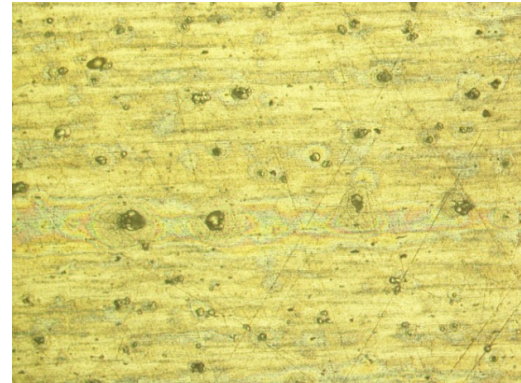
Metallographic investigations at various magnification levels were conducted in order to study the effect of tilt angle on the evolved microstructure of the joints. It has been observed from the findings in the past<sup>24</sup> that the





**Figure 7.** Test coupon welded at  $1^\circ$  tool tilt angle.

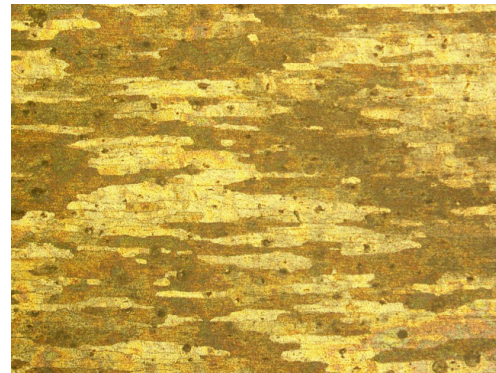
transverse cross-section around the joint line can be divided into four zones: (1) the unchanged parent metal zone - region away from the weld; (2) the heat affected zone (HAZ) - region where the material is subjected to a thermal cycle that has altered the mechanical and/or the microstructure properties; (3) the thermo-mechanically affected zone (TMAZ) - region where plastic deformation takes place due to the action of the the FSW tool; and (4) weld nugget (WN) - region where recrystallation takes place by the tool pin. Table 5 shows the microstructures of FS welded joints obtained under varied welding conditions. The three major zones viz. the WN zone, AS-TMAZ (advancing-TMAZ), and RS-TMAZ (retreating-TMAZ), are shown in Table 5. Column 2 of table 5 shows the centre of the WN zones. The metallographic investigation shows that both the AS-TMAZ and RS-TMAZ have a boundary with the WN. Critical observations showed that interface between the WN and TMAZ in the advancing side is more clearly visible than that on the retreating side. The microstructure analysis of all the joints except the joint fabricated with  $2^\circ$  showed defects. The test coupon welded with  $2^\circ$  tilt angle was found to be a sound weld without any micro defects. Column 5 in table 5 shows the weld defects resulting from FSW under different tilt angles. The defects can be mainly classified as voids and unfilled regions. The defects were largely observed in bottom half of the advancing side. The investigation of the defects shows that the location, shape and size of the defect changes with change in the tool tilt angle. The microstructure of the base material Al 7075 T651 is shown in Figure 8(a). Figures 8(b) to 8(d) shows WN, TMAZ and HAZ zones for sample C respectively. The three zones viz. WN, TMAZ and HAZ are easily identified by their microstructures.



**Figure 8 (a).** Base material (200X).



**Figure 8 (b).** Weld nugget zone (200X).



**Figure 8 (c).** Thermomechanically affected zone (200X).

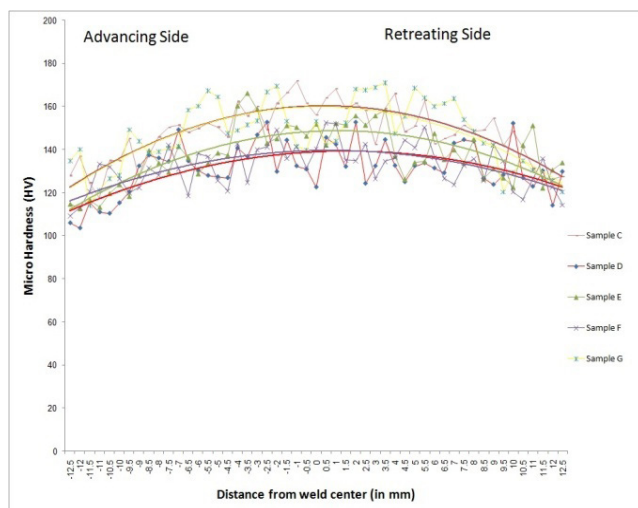


**Figure 8 (d).** Heat affected zone (200X).

Figure 8(a) depicts the microstructure of the parent metal comprising of insoluble second phase precipitates scattered in different areas. The grains are elongated in the rolling direction. Figure 8(b) evidently shows that FSW transforms the flat grains in the parent metal to fine-equiaxed recrystallized grains in the WN zone. This is a effect of elevated temperature and high rate of stirring action by the virtue of the tool pin. The bending of the grains in the thermo mechanically affected zone is due to the plastic deformation caused by the stirring action of the tool. The TMAZ is shown in Figure 8(c). The HAZ is the region where there no plastic deformation at all; the zone is significantly the result of frictional heating of the tool shoulder. Figure 8(d) indicates that in the HAZ the grain structure and the flow pattern did not significantly alter.

### 3.3 Microhardness Results

The microhardness was measured in the center of the welds in the transverse direction. The measurement was done in the WN zone and the TMAZ. FSW results in coarsening and coarsening/dissolution of the initial hardening precipitates in the WN and TMAZ. This effect tend to reduce the hardness in the WN zone and the surrounding regions. In the present study also the weld nugget zone recorded higher values of hardness than compared to the TMAZ. Figure 9 shows the hardness distributions in different samples. The left portion of the profile shows the hardness distribution on the advancing side and the right part shows that of the retreating side.



**Figure 9.** Effect of tool tilt angle on microhardness of Al 7075-T651 aluminium alloy.

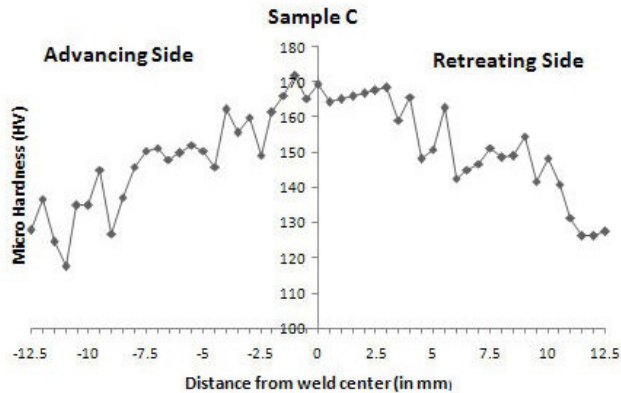
The microhardness in the TMAZ and the WN were observed to be lower than the hardness of the base metal. The finer grain size in the WN zone compared to other regions being the main reason for this. As per the Hall-Petch equation, the hardness increases as the grain size decreases. A noteworthy reduction in the hardness value is seen in the TMAZ. This is because of the coarsening of the precipitates in the thermo mechanically affected zone. The minimum in the hardness was observed to be at around 12 mm on either side. Similar kind of observations have been made by Rajakumar et al.<sup>4</sup> From Figure 9 it is additionally revealed that there is a slight asymmetry in hardness values between the retreating side and the advancing side. The non uniform plastic flow resulting due to FSW is the major cause for the asymmetry in the hardness. In order to predict the behavior of the hardness data, a trend line is plotted for each of the hardness values. The trend line clearly depicts that the hardness values on the advancing side are lower compared to the retreating side for welding done with any tool tilt angles used. The maximum hardness was found to be of the sample C. Figure 10 shows the hardness distributions for sample C. The weld nugget zone recorded higher values of hardness than compared to other regions. The hardness in the weld nugget zone is in the range of 160 to 170 HV. It has been revealed in the literature available that the hardness measured on the cross-section perpendicular to the welding direction for friction stir welded heat-treatable aluminium alloys (in T6 or T7 temper condition) typically represents a “W-shaped” curve<sup>25-28</sup>. Figure 10 shows a typical “W-shaped” curve representing the hardness profile for sample C. Here, the hardness profile of all sample have exhibited the “W-shaped” curve.

### 3.4 Tensile strength properties and fracture locations

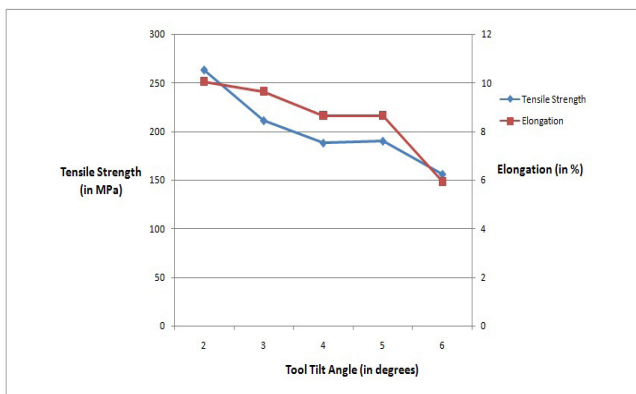
The transverse tensile strength tests of all the welds were undertaken. From each weld coupon, three specimens were tested. The average tensile strengths and percentage elongations of the three samples are presented in Table 6. The maximum joint strength was exhibited by the weld made at 2° tool tilt angle. The maximum strength of the weld was 263MPa with an elongation of 10.06%. The tensile strength and the elongation were observed to decrease with the increase in tool tilt angle. It has been observed that when the tool tilt angle is greater than 3° the tensile properties of the joints decreases to considerably low lev-



els. The same is reflected in Figure 11. Additionally it was also observed that apart from sample C which failed in the TMAZ of AS, all the other joints failed in the WN zone.



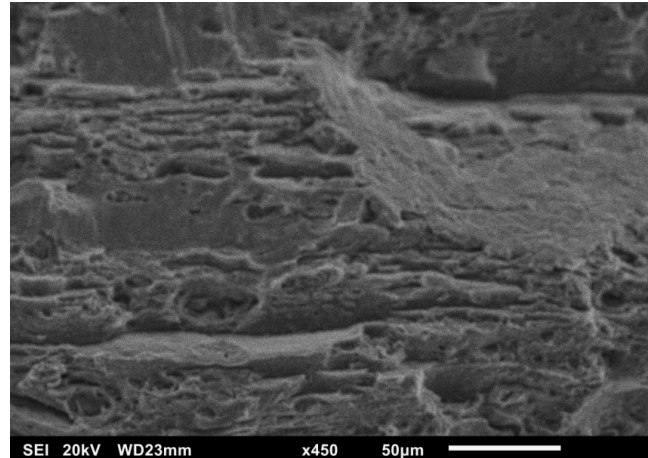
**Figure 10.** Hardness profile across the weld made with 20 tool tilt angle.



**Figure 11.** Transverse tensile strength properties of the welded joints.

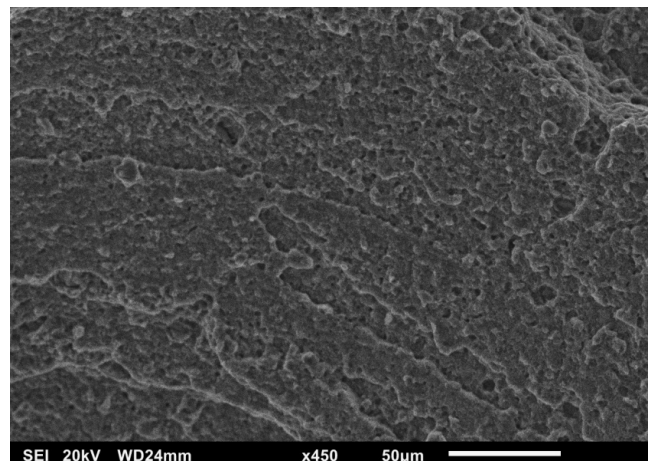
### 3.5 Fractography

It is certain that the fusion welded heat treatable aluminum alloys are accompanied by welding defects like porosities and inclusions<sup>29</sup>. FSW takes place in solid. Hence FSW joints are free from such defects. The major defects that FSW joints are prone to are excessive flash, voids, wormholes, excessive concavity, lack of penetration, and kissing bond defects. SEM is used to study the failure patterns of the fracture surface of the tensile specimens. Figure 12 shows the fracture surface of the unwelded parent metal indicating an approximately equiaxed pattern and confirms the superior mechanical properties of the joint. It reveals that the specimen has failed in pure tensile mode.



**Figure 12.** SEM micrograph of fracture plane of Al 7075-T651 parent metal.

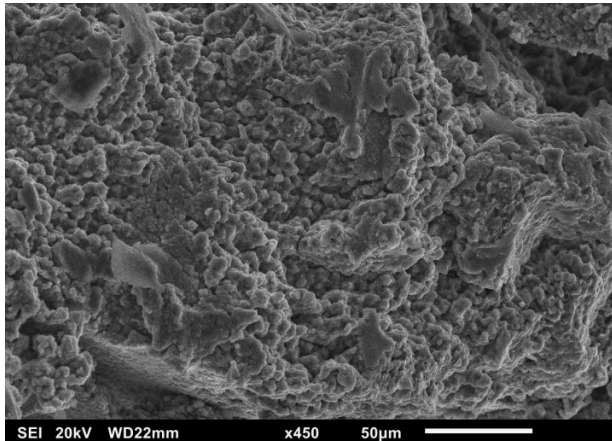
The fracture surfaces of the welded specimens (viz. samples C, D, E, F and G) have been captured and are shown as Figures 13 -17. Microstructure analysis showed that sample C had no weld defect hence the failure of tensile specimens for sample C was in the TMAZ away from the weld nugget zone. Whereas the presence of defects in the weld nugget zone of the other joints is the major reason for the failure of these joints. Figure 13 shows fracture surface of sample C with the presence of pits defining a ductile mode of fracture.



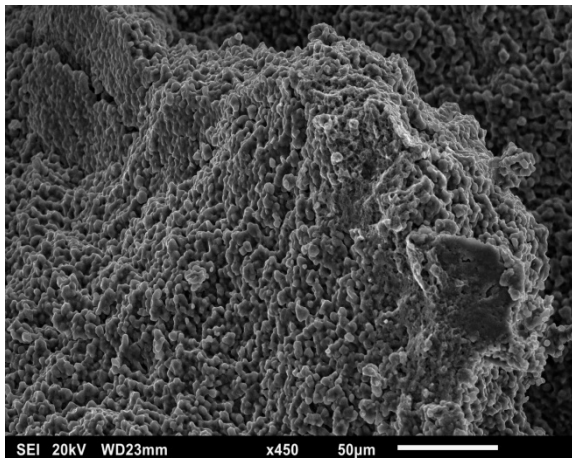
**Figure 13.** SEM micrograph of fracture plane of joint welded with 2° tilt angle.

On the contrary, a brittle fracture is found in all the other joints. Fracture surfaces (Ref. Figures 14 - 17) observed under SEM for the samples D,E,F and G shows an uneven surface accompanied with fibrous tedious

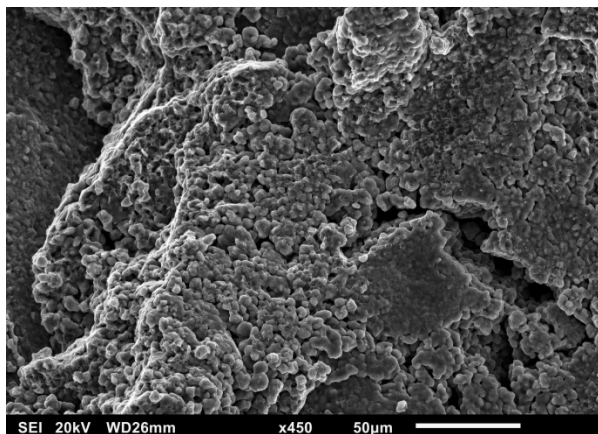
appearance which are clearly characteristics of a brittle fracture.



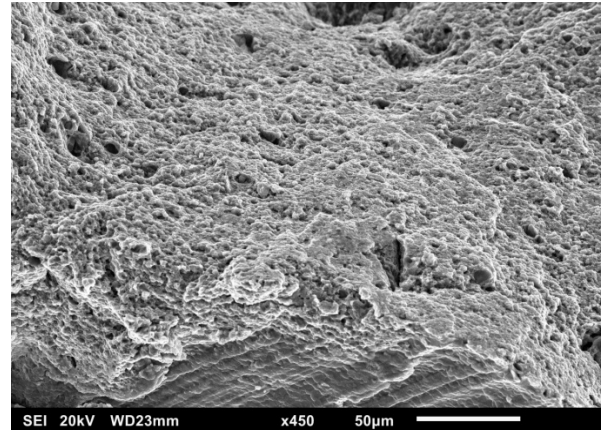
**Figure 14.** SEM micrograph of fracture plane of joint welded with 4° tilt angle.



**Figure 15.** SEM micrograph of fracture plane of joint welded with 4° tilt angle.



**Figure 16.** SEM micrograph of fracture plane of joint welded with 50° tilt angle.



**Figure 17.** SEM micrograph of fracture plane of joint welded with 6° tilt angle.

**Table 4.** Friction stir welding parameters

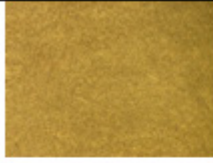


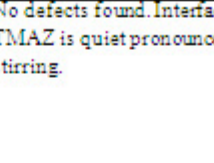

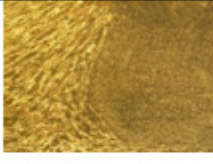



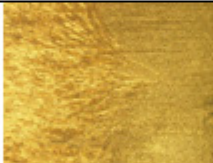
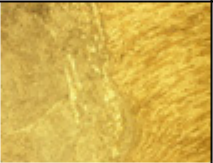
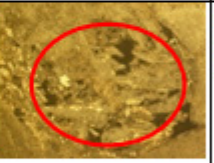

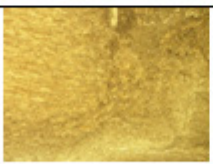
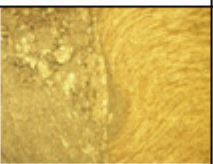
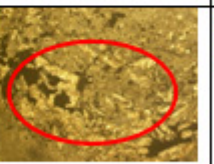
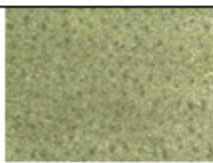
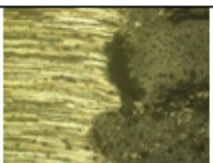
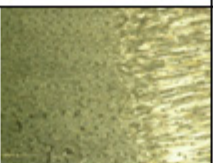

Sample ID	Tool Rotation Speed (in rpm)	Welding Speed (in mm/min)	Tool Tilt Angle (in degrees)
A	1500	50	0°
B			1°
C			2°
D			3°
E			4°
F			5°
G			6°

#### 4. Results and Discussion

Al 7075 T651 is a precipitation hardenable alloy as other 7XXX series are. It shows a marked response to precipitation hardening. The precipitates are observed under various forms. The precipitation process initiates with the formation of GP zones in the temperature range of 120 - 135°C followed by the formation of  $\eta'$  Mg(Zn, Cu, Al)<sub>2</sub> phase at around 160 - 170°C. The metastable  $\eta'$  stage precedes the formation of  $\eta$  phase which takes place at around 200°C. Modification in the metastable state during welding reduces the strength of the weldment<sup>11,30</sup>. Previous studies have shown that the temperature that prevails at the edge of the weld nugget varies from 422°C to 475°C during FSW of Al 7075 T651 alloys<sup>9</sup>. The solutionizing temperature is quite lower than the temperature in the weld region. These high temperatures exist for a very short duration but long enough to affect the strengthening precipitate morphology. The strengthening precipitates tend to dissolve in the matrix at such high temperatures



**Table 5.** Microstructural analysis of samples welded with different tool tilt angles

Sample ID (1)	Stir (Nugget) Zone (2)	Advancing Side (WN - TMAZ) (3)	Retreating Side (WN - TMAZ) (4)	Micrographs of Defects (5)	Name of the Defects and its location (6)
C					No defects found. Interface between WN and TMAZ is quite pronounced indicating proper stirring.
D					Tunnel Defect in the advancing side.
E					Internal Cavity (Open Voids) in the stir zone.
F					Internal Cavity (Open Voids) in the stir zone.
G					Internal Cavity (Open Voids) in the stir zone. (Weak linkage between WN and TMAZ indicating improper stirring)

resulting in inferior mechanical strength of the resulting joint. This phenomena alongwith the defects found in the weld nugget zone are the major reasons for the inferior mechanical strength of the welded joints under the current investigation.

**Table 6.** Tensile properties of friction stir welds

Sample ID	Ultimate Tensile Strength (MPa)	Elongation (%)
C	263	10.06
D	211	9.67
E	188	8.67
F	190	8.67
G	156	5.96

For the present study the minimum hardness was found to be at about 12 mm on either side and the maxi-

imum hardness of about 160 -170 HV was noted in the WN zone. The major reason for this observed phenomenon might be the fact that dissolution is favoured both in the and WN and TMAZ during the process as a result of high temperature and strain rates. Whereas in the HAZ no plastic deformation is observed and the temperatures are considerably lower than the dissolution temperature of the precipitates. Hence HAZ is characterized by coarsening of initial hardening precipitates. The tendency to coarsen is much higher at the grain boundaries resulting in a precipitate free zone at and near the grain boundaries. This can be the major reason of sample C (no defects) getting failed outside the weld nugget. Whereas all the other joints have failed within the WN zone due to the weld defects. The size of the defects have increased with an increase in the tool tilt angle. The major reason for this can be attributed to the fact that, with an increase in

the tilt angle (with pin length kept constant), the bottom end of the pin lifts up more from the root of the weld. This results in insufficient material flow during welding creating the unfilled regions. Subsequently the tensile strengths also decreased with the increase in tool tilt angle and above a tilt angle greater than  $3^\circ$ , the tensile properties of the joints decreased to considerably low levels. The occurring of this phenomena is clearly observed from the micrographs shown in Table 5. Columns 3 and 4 in the Table 5 shows that the interface between the weld nugget and the TMAZ is quiet pronounced in the samples welded with  $2^\circ$  and  $3^\circ$  tilt angle. Whereas for the samples welded above  $3^\circ$ , the interface is not clearly visible indicating improper stirring of the material above  $3^\circ$  tilt angle.

## 5. Conclusions

The present investigation is specifically aimed to understand the influence of tool tilt angle in regards to the mechanical properties and microstructural development of the joints formed during the process. Its reveals the following:

- The joint fabricated with  $2^\circ$  tool tilt angle yielded highest strength properties.
- The maximum UTS reported at  $2^\circ$  tool tilt angle is 263 MPa.
- Generally the defect free weld specimen fails in the minimum hardness zone. But in the present investigation most of the joints (except sample welded with  $2^\circ$  tool tilt angle) have failed in the WN mainly because of the defects present in the WN zones.
- The SEM images revealed that the joints welded with  $2^\circ$  tool tilt angle failed with a ductile mode of fracture, whereas the joints welded with other tilt angles failed with a brittle mode of fracture during the tensile test.
- Although reduction in strength properties are observed, FSW offers potential for welding 7075-T651 aluminum alloys.

## 6. Acknowledgements

The work was supported by Indian Space Research Organisation (ISRO), India. The authors would like to express their gratitude to ISRO for rendering financial aid through a R&D Project No. E33011/60/2010-V.

## 7. References

1. Rajakumar S, Muralidharan C, Balasubramanian V. Influence of friction stir welding process and tool parameters on strength properties of AA7075-T6 aluminium alloy joints. *Materials and Design*. 2011; 32(2):535–549.
2. Sivaraj P, Kanagarajan D, Balasubramanian V. Effect of post weld heat treatment on tensile properties and microstructure characteristics of friction stir welded armour grade AA7075-T651 aluminium alloy. *Defence Technology*. 2014; 10(1):1–8.
3. Shtrikman MM. Trends in the development of the friction stir welding process. *Welding International*. 2015; 29(3):230–239.
4. Cam G, Mistikoglu S. Recent developments in friction stir welding of al-alloys. *Journal of Materials Engineering and Performance*. 2014; 23(6):1936–1953.
5. Shah PH, Badheka V. 3rd International Conference on Innovations in Automation and Mechatronics Engineering 2016, ICIAME 2016 05-06 February, 2016. An experimental investigation of temperature distribution and joint properties of Al 7075 T651 friction stir welded aluminium alloys. *Procedia Technology*. 2016; 23: p. 543–550.
6. Fuller CB, Mahoney MW, Calabrese M, Micono L. Evolution of microstructure and mechanical properties in naturally aged 7050 and 7075 Al friction stir welds. *Materials Science and Engineering: A*. 2010; 527(9):2233–2240.
7. Mahoney MW, Rhodes CG, Flintoff JG, Bingel WH, Spurling RA. Properties of friction-stir-welded 7075 T651 aluminum. *Metallurgical and Materials Transactions A*. 1998; 29(7):1955–1964.
8. Rhodes CG, Mahoney MW, Bingel WH, Spurling RA, Bampton CC. Effects of friction stir welding on microstructure of 7075 aluminum. *Scripta Materialia*. 1997; 36(1):69–75.
9. Fratini L, Buffa G, Shivpuri R. Mechanical and metallurgical effects of in process cooling during friction stir welding of AA7075-T6 butt joints. *Acta Materialia*. 2010; 58(6):2056–2067.
10. da Silva AAM, Arruti E, Janeiro G, Aldanondo E, Alvarez P, Echeverria A. Material flow and mechanical behaviour of dissimilar AA2024-T3 and AA7075-T6 aluminium alloys friction stir welds. *Materials and Design*. 2011; 32(4):2021–2027.
11. Singh RKR, Sharma C, Dwivedi DK, Mehta NK, Kumar P. The microstructure and mechanical properties of friction stir welded Al–Zn–Mg alloy in as welded and heat treated conditions. *Materials and Design*. 2011; 32(2):682–687.
12. Zhao Y, Wang Q, Chen H, Yan K. Microstructure and mechanical properties of spray formed 7055 aluminum alloy by underwater friction stir welding. *Materials and Design*. 2014; 56(0): 725–730.

13. Dieguez T, Burgueño A, Svoboda H. Superplasticity of a Friction Stir Processed 7075-T651 Aluminum Alloy. *Procedia Materials Science*. 2012; 1(0):110–117.
14. Patel VV, Badheka V, Kumar A. Effect of polygonal pin profiles on friction stir processed superplasticity of AA7075 alloy. *Journal of Materials Processing Technology*. 2017; 240:68–76.
15. Ma ZY, Mishra RS, Mahoney MW. Superplastic deformation behaviour of friction stir processed 7075Al alloy. *Acta Materialia*. 2002; 50(17):4419–4430.
16. García-Bernal MA, Mishra RS, Verma R, Hernández-Silva D. Influence of friction stir processing tool design on microstructure and superplastic behavior of Al-Mg alloys. *Materials Science and Engineering: A*. 2016; 670: p. 9–16.
17. Sharma C, Dwivedi DK, Kumar P. Effect of post weld heat treatments on microstructure and mechanical properties of friction stir welded joints of Al–Zn–Mg alloy AA7039. *Materials and Design*. 2013; 43(0):134–143.
18. Dilip Raja N, Velu R, Selvamani ST. An experimental study of mechanical properties and effect of welding speed of friction stir welding on aluminium alloy 6061. *Indian Journal of Science and Technology*. 2015; 8(35):1–7.
19. Reynolds AP, Lockwood WD, Seidel TU. Processing-Property correlation in friction stir welds. *Materials Science Forum*. 2000; 331-337:1719–1724.
20. Hatamleh O, Lyons J, Forman R. Laser and shot peening effects on fatigue crack growth in friction stir welded 7075-T7351 aluminum alloy joints. *International Journal of Fatigue*. 2007; 29 (3):421–434.
21. Hatamleh O. The effects of laser peening and shot peening on mechanical properties in friction stir welded 7075-t7351 aluminum. *Journal of Materials Engineering and Performance*. 2008; 17(5):688–694.
22. Kumaraswami Dhas LA, Raguraman D, Muruganandam D, Senthilkumar B. Temperature prediction using finite element modeling on friction stir welding of AA6061-AZ61. *Indian Journal of Science and Technology*. 2015; 8(31):1–7.
23. Feng AH, Chen DL, Ma ZY. Microstructure and cyclic deformation behavior of a friction-stir-welded 7075 Al Alloy. *Metallurgical and Materials Transactions A*. 2010; 41(4):957–971.
24. Hwang Y-M, Kang Z-W, Chiou Y-C, Hsu H-H. Experimental study on temperature distributions within the work-piece during friction stir welding of aluminum alloys. *International Journal of Machine Tools and Manufacture*. 2008; 48(7–8):778–787.
25. Denquin D A, Campagnac MH and Lapasset G. Microstructural and mechanical evolutions within friction stir welds of precipitation hardened aluminium alloys materials science forum. 2003; 426-432:2921–2926.
26. Reshad Seighalani K, Besharati Givi MK, Nasiri AM, Bahemmat P. Investigations on the effects of the tool material, geometry, and tilt angle on friction stir welding of pure titanium. *Journal of Materials Engineering and Performance*. 2010; 19(7):955–962.
27. Gan W-y, Zhou Z, Zhang H, Peng T. Evolution of microstructure and hardness of aluminum after friction stir processing. *Transactions of Nonferrous Metals Society of China*. 2014; 24(4):975–981.
28. Fonda RW, Bingert JF. Precipitation and grain refinement in a 2195 Al friction stir weld. *metallurgical and materials transactions A*. 2006; 37(12):3593–3604.
29. Gurvir SS, Gurmeet K, Singh B. Analysis of micro vickers hardness of friction stir welding of dissimilar aluminum alloys (AA6061-T6 and AA6082-T6). *Indian Journal of Science and Technology*. 2016; 9(36):1–3.
30. Kumar K, Kailas SV, Srivatsan TS. Influence of tool geometry in friction stir welding. *materials and manufacturing processes*. 2008; 23(2):188–194.